Characterization of Edge Effects With Paclitaxel-Eluting Stents Using Serial Intravascular Ultrasound Radiofrequency Data Analysis: The BETAX (BEside TAXus) Study

Héctor M. García-García, Nieves Gonzalo, Shuzou Tanimoto, Emanuele Meliga, Peter de Jaegere, and Patrick W. Serruys

Thoraxcenter, Erasmus MC, Rotterdam, The Netherlands

Introduction and objectives. At present, the effect of paclitaxel on tissue structure at the edges of Taxus® stents is unknown. The objective of this study was to investigate in vivo the temporal changes occurring at the edges of paclitaxel-eluting stents using intravascular ultrasound radiofrequency (IVUS-RF) data analysis.

Methods. The study included 24 patients who had a total of 26 paclitaxel-eluting stented segments. In all patients, IVUS-RF imaging was performed 5 mm proximally and 5 mm distally to the stent edges 6 months after stent implantation. For subsequent analysis, proximal and distal segments were divided into five 1-mm subsegments.

Results. In the first 2 subsegments adjacent to the proximal edge of the stent, the vessel wall had grown to compensate for plaque growth without affecting the vessel lumen, while in the remaining three subsegments there was overcompensation (ie, the vessel wall increased to greater than the plaque size). Consequently, the lumen had increased in size. At the distal edge of the stent, overcompensation was observed in all five subsegments and the lumen had increased in size. In general, proximal and distal growth was due to an increase in fibrolipid plaque (P<.001 and P<.001, respectively) along with a decrease in the necrotic core (P=.014 and P<.001, respectively) and the presence of dense calcium (P<.001 and P<.001, respectively).

Conclusions. Serial expansive vascular remodeling was observed at proximal and distal stent edges. Remodeling occurred in response to tissue growth, which was mainly due to increased fibrofatty tissue.

Key words: *Restenosis. Imaging. Drug-eluting stents. Coronary disease.*

SEE EDITORIAL ON PAGES 1001-6

Correspondence: Dr. P.W. Serruys,
Thoraxcenter, Bd583a,
Dr. Molewaterplein 40, 3015-GD, Rotterdam, The Netherlands
E-mail:p.w.j.c.serruys@erasmusmc.nl

Received November 30, 2007.
Accepted for publication March 13, 2008.

Caracterización de los efectos tisulares en los segmentos adyacentes a los stents liberadores de paclitaxel según el análisis de datos de radiofrecuencia procedentes de ecocardiografía intravascular seriada: estudio BETAX (BEside TAXus)

Introducción y objetivos. En la actualidad se desconoce el efecto de paclitaxel en la composición tisular en los segmentos adyacentes (bordes) del *stent* Taxus®. El objetivo de este estudio fue investigar in vivo los cambios temporales que se producen en los bordes del *stent* liberador de paclitaxel según un análisis de los datos de radiofrecuencia procedentes de ecografía intravascular (EIV).

Métodos. En total participaron 24 pacientes (26 segmentos con *stents* liberadores de paclitaxel). Se obtuvieron imágenes con EIV de los 5 mm proximales y los 5 mm distales de los bordes del *stent* transcurridos 6 meses del implante. Para realizar un análisis posterior, los segmentos proximales y distales se fraccionaron en cinco subsegmentos de 1 mm cada uno.

Resultados. En los primeros dos subsegmentos adyacentes al *stent* del borde proximal, la pared del vaso crece para compensar el crecimiento de la placa sin que ello afecte a la luz, mientras en los siguientes 3 subsegmentos se observó una sobrecompensación (la pared del vaso aumentó más que el tamaño de la placa). Por lo tanto, aumentó el tamaño luminal. En el borde distal, se observó sobrecompensación en todos los subsegmentos, seguida de un aumento del tamaño luminal. En general, el crecimiento proximal y distal se basó en un aumento de la placa fibrolipídica ($p < 0,001$ y $p < 0,001$ respectivamente), con una disminución del núcleo necrótico ($p = 0,014$ y $p < 0,001$ respectivamente) y un contenido denso de calcio ($p < 0,001$ y $p < 0,001$ respectivamente).

Conclusiones. Se observó un remodelado vascular expansivo y seriado en los bordes proximal y distal del *stent,* para acomodar un crecimiento tisular principalmente debido al aumento del tejido fibrolipídico.

Palabras clave: *Reestenosis. Técnicas de imagen.* Stents *farmacoactivos. Enfermedad coronaria.*

ABREVIATIONS

CSA: cross-sectional area
IVUS: intravascular ultrasound
RFD: radiofrequency data

INTRODUCTION

Stent use has been one of the major breakthroughs in the treatment of patients with coronary artery disease.[1] Together with its many advantages some associated pitfalls are restenosis and stent thrombosis.[2-9] Regarding the vascular responses after stenting (ie, restenosis and remodeling), a response-to-injury pattern of wound healing occurs, mainly characterized by an increase in smooth muscle cells and extracellular matrix.[10]

In the Taxus II study a significant reduction in lumen size was observed at the proximal edge in both paclitaxel eluting stent and bare metal stent groups, while at the distal edge the reduction was only present in the bare metal stent group. This was mainly due to an augment in plaque size not fully compensated by vessel wall remodeling.[11]

Nowadays spectral analysis of the intravascular ultrasound (IVUS) radiofrequency data (RFD) analysis[12,13] is emerging as a tool to assess tissue composition in the coronary arteries. Thus, not only serial geometrical changes can be analyzed, but also its composition.

However, in stented vessels this can only be performed at the edges of the stent, because the actual stent area and its surroundings cannot be analyzed with IVUS-RFD, due to: *a)* misclassification of the stent struts as "dense calcium"; *b)* lack of proper validation of IVUS-RFD in this context; and *c)* potential interference of the superficial stent struts on the backscattering of the tissue behind them.

We hypothesized that the tissue involved in the increase of plaque at the stent edges, as assessed by IVUS-RFD, is mainly fibro-fatty tissue, which has been described as loosely packed bundles of collagen fibers with regions of lipid deposit and extracellular matrix without necrotic areas.[14]

We thus sought in vivo the temporal geometrical and tissue composition changes at the edge of paclitaxel-eluting stent as assessed by IVUS-RFD analysis.

METHODS

Patient Selection

The BEside TAXus® (BETAX) study was a longitudinal and prospective cohort of non-consecutive patients who had a clinical indication for coronary intervention and were treated with Taxus® stent (Taxus® Express^{2TM}; Boston Corporation, Natick, MA, USA) in at least one of their coronary arteries. Only patients who gave informed written consent were included in the study. Patients with stable angina and acute coronary syndromes were included. Acute coronary syndromes comprise unstable angina, non-ST segment elevation myocardial infarction and ST-segment elevation myocardial infarction. IVUS-RFD imaging was performed at post-stenting and at 6 months. Our local Ethics Committee approved the protocol.

IVUS-RFD Acquisition and Analysis

Details regarding the validation of the technique, on explanted human coronary segments and in vivo post-atherectomy, have been previously reported.[12-14] Briefly, IVUS-RFD uses spectral analysis of IVUS radiofrequency data to construct tissue maps that are correlated with a specific spectrum of the radiofrequency signal and assigned color codes (fibrous [labeled green], fibrofatty [labeled greenish-yellow], necrotic core [labeled red], and dense calcium [labeled white]).[12,13]

IVUS-RFD was acquired using a continuous pullback (Eagle-Eye^{TM} 20 MHz Volcano Therapeutics, Rancho Cordova, CA, USA) by a dedicated IVUS-RFD console (Volcano Therapeutics, Rancho Cordova, CA, USA). The IVUS-RFD recordings were stored on a DVD and sent to Corelab (Erasmus Medical Center/Cardialysis, Rotterdam, The Netherlands) for offline analysis.

The 5-mm proximal (p) and 5-mm distal (d) segments adjacent to the stent were subsequently divided into 1-mm 5 subsegments (ss) (Figure).

The IVUS-RFD sampling rate during pullback is gated to peak R-wave and is therefore dependent on heart rate. For instance, during constant heart rate of 60 bpm, data will be collected every 0.5 mm.

Compositional and geometrical data were obtained for every cross-sectional area (CSA) and expressed as mean areas and percent for each IVUS-RFD component.

Statistical Analysis

Discrete variables are presented as counts and percentages. Continuous variables are presented as means (SD). A *P* value (2-sided) less than .05 was considered significant. Assumptions for normality were checked after transformation based on a *P* value >.20 at Kolmogorov-Smirnov test and by visual assessment of Q-Q plots of residuals. Accordingly, log transformation was performed on the variables with skewed distribution.

The comparison between baseline and follow-up was performed using paired Student *t* test.

Statistical analyses were performed with use of SPSS software version 11.5.

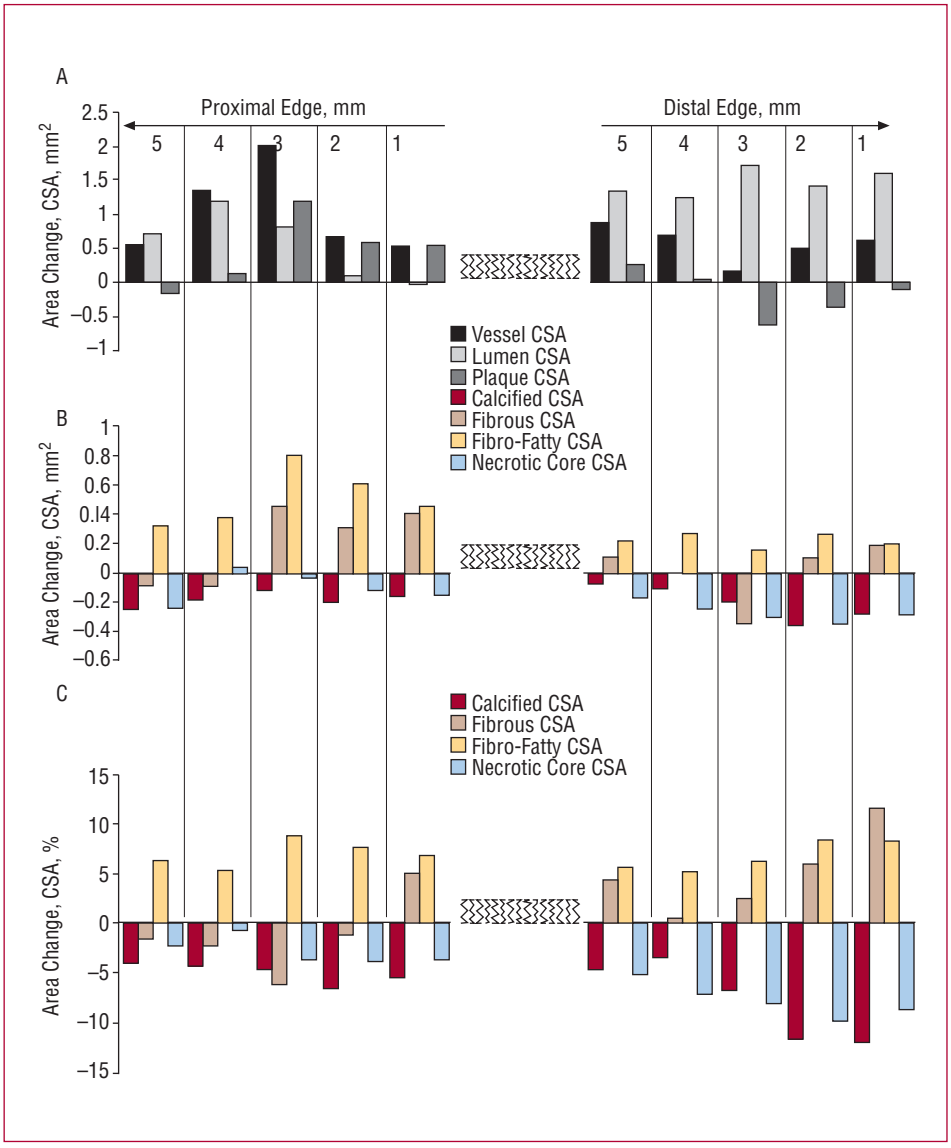

Figure. A: area changes in geometrical measurements at the proximal and distal 5-mm of the Taxus stent. B and C: absolute and relative temporal changes in plaque composition. CSA indicates cross-sectional area.

RESULTS

Overall, 30 patients were included in this study, but only 24 (26 stented segments) patients were ultimately analyzed. Two patients refused angiographic follow-up and in other 4 patients the IVUS image quality was poor (non-continuous pullback and presence of IVUS artifacts). The baseline characteristics of the patient population are depicted in Table 1. The mean age was 57.6 (11.2) years, most being male patients (75%) and 66% of the patients presented with stable angina. The studied vessel was the left anterior descending artery in 46.2 %, the left circumflex in 26.9 %, and the right coronary artery in 26.9 % of the cases. The mean number of stent per patient was 1.5 (0.7). No stent thrombosis has been observed so far.

IVUS-RFD Findings. Changes From Baseline to Follow-up in Geometrical and Compositional Parameters Within and Between the Proximal and Distal Segments.

At baseline, the mean vessel CSA (16.5 [4.9] vs 11.5 [4.0] mm^2; $P<.001$), plaque CSA (7.7 [3.6] vs 5.3 [2.7] mm^2; $P<.001$), and lumen CSA (8.8 [2.6] vs 6.2 [1.7] mm^2; $P<.001$) of the entire 5-mm edge segment in the proximal edge were larger than their counterparts in the distal segment. The same holds at follow-up for the measurements of the mean vessel CSA (17.5 [5.9] vs 12.8 [4.0] mm^2; $P<.001$), plaque CSA (8.2 [4.4] vs 5.1 [2.6] mm^2; $P<.001$), and lumen CSA (9.3 [3.0] vs 7.7 [4.0] mm^2; $P<.001$) (Table 2).

TABLE 1. **Demographic, Medication, and Procedure Characterisitics (n=24)**

Age, mean (SD), y	57.6 (11.2)
BMI, mean (SD), kg/m^2	28.1 (3.8)
Male 18	(75)
Hypertension	10 (41.7)
Diabetes mellitus	6 (25)
Hypercholesterolemia	10 (41.7)
Current smoker	4 (16.7)
Previous cardiac history	5 (20.8)
Previous CABG	0
Previous ACS	3 (12.5)
Family history of CAD	11 (45.8)
Clinical presentation	
Stable angina	16 (66.6)
ACS	9 (37.4)
Medication	
Aspirin	
Baseline	17 (70.8)
6 Months follow-up	24 (100)
Clopidogrel	
Baseline	5 (20.8)
6 Months follow-up	24 (100)
Beta-blockers	
Baseline	7 (29.2)
6 Months follow-up	19 (79.2)
ACE inhibitor	
Baseline	5 (20.8)
6 Months follow-up	12 (50)
Calcium channel blocker	
Baseline	3 (12.5)
6 Months follow-up	1 (4.2)
Statins	
Baseline	12 (50)
6 Months follow-up	21 (87.5)
Studied vessel (n=26)	
LAD	12 (46.2)
LCX	7 (26.9)
RCA	7 (26.9)
Procedure characteristics	
Stent length, mean (SD), mm	16.6 (4.1)
Stent diameter, mean (SD), mm	3 (0.41)
Balloon pre-dilatation	11 (42.3)
Balloon length/stent length ratio, mean (SD)	0.97 (0.27)
Stent implantation pressure, mean (SD), atm	19.6 (3.24)

ACS indicates acute coronary syndrome; BMI, body mass index; CABG, coronary artery bypass graft; CAD, coronary artery disease; LAD, left anterior descending; LCX, left circumflex; RCA, right coronary artery.
Data are expressed as n (%) or median (SD).

TABLE 2. **IVUS Virtual Histology Tissue Composition and Geometrical Data in the Entire 5 mm Segments**

	Calcified, mm^2	Calcified, %	Fibrotic, mm^2	Fibrotic, %	Fibrofatty, mm^2	Fibrofatty, %	Necrotic Core, mm^2	Necrotic Core, %	Vessel Cross Sectional Area, mm^2	Lumen Cross Sectional Area, mm^2	Plaque Cross Sectional Area, mm^2	Plaque Burden, %
Proximal edge												
Baseline	0.52 (0.63)	10.7 (11.5)	2.6 (2.1)	57.9 (19.3)	0.52 (0.71)	11.7 (11.9)	0.74 (0.69)	17 (13.5)	16.5 (4.9)	8.8 (2.6)	7.7 (3.6)	45.4 (11.9)
Follow-up	0.32 (0.49)	5.8 (8.2)	2.8 (2.5)	56.9 (18.4)	1.02 (1.15)	18.7 (13.4)	0.63 (0.77)	14.2 (13.8)	17.5 (5.9)	9.3 (3)	8.2 (4.4)	45.1 (12.6)
P	<.0001	<.001	.48	.49	<.001	<.001	.014	.002	.031	.043	.54	.95
Distal Edge												
Baseline	0.29 (0.48)	11 (14.2)	1.4 (1.4)	47.8 (29.2)	0.21 (0.33)	7 (9.3)	0.52 (0.86)	18.5 (16.5)	11.5 (4)	6.2 (1.7)	5.3 (2.7)	43.5 (10)
Follow-up	0.09 (0.17)	3.3 (6.3)	1.4 (1.4)	53 (28.7)	0.43 (0.54)	13.7 (13.1)	0.26 (0.32)	10.8 (12.6)	12.8 (4)	7.7 (4)	5.1 (2.6)	40.2 (10.7)
P	<.001	<.001	.99	.18	<.001	<.001	<.001	<.001	.063	<.001	.69	.001
Baseline												
Proximal versus distal edge, *P*	<.001	.8	<.001	<.001	<.001	<.001	<.001	.23	<.001	<.001	<.001	.038
Follow-up												
Proximal versus distal edge, *P*	<.001	<.001	<.001	<.001	<.001	<.001	<.001	<.001	<.001	<.001	<.001	<.001

At the proximal and distal edges, a serial expansive vascular remodeling was observed at follow-up, with a significant increase in mean vessel CSA of the entire proximal (*P*=.031) and trend towards an increase in the distal segment (*P*=.06).

Since plaque CSA hardly increases, this remodeling resulted in a significant increase in mean lumen CSA was observed (Table 2).

In terms of tissue composition, at baseline, in the proximal segment as compared to the distal, the percentage of calcified tissue was not different (10.7% [11.5%] vs 11.0% [14.2%]; *P*=.80), the same was true for the necrotic core (17.0% [13.5%] vs 18.5% [16.5%]; *P*=.23); on the contrary significantly larger percentage of fibrous (57.9% [19.3%] vs 47.8% [29.2%]; *P*<.001), and fibrofatty tissue (11.7% [11.9%] vs 7.0% [9.3%]; *P*<.001) were observed.

At follow-up, all tissue types were larger in the proximal segment than in the distal, calcified (5.8% [8.2%] vs 3.3% [6.3%]; *P*<.001), necrotic core (14.2% [13.8%] vs 10.8% [12.6%]; *P*<.001), fibrous (56.9% [18.4] vs 53.0% [28.7%]; *P*<.001), and fibrofatty tissue (18.7% [13.4%] vs 13.7% [13.1%]; *P*<.001) (Table 2).

Overall, in the proximal and distal segments a significant increase of fibrofatty tissue was observed, whereas a decrease of calcified and necrotic core over the time was present. Fibrous tissue did not show significant temporal changes (Table 2).

Subsegmental Analysis of Longitudinal Changes at 5-mm Edge Segment of Proximal and Distal Edges

The mean absolute difference vessel CSA (follow-up – baseline) was positive throughout the proximal and distal segments; this was accompanied by a positive mean absolute difference in lumen CSA; the most prominent increase in plaque CSA (although not significant) was documented in first three proximal subsegments. (Figure). In particular, at the proximal edge, in the first 2 millimeters the vessel wall grew to compensate for the plaque growth (1-mm pss, Δ+0.52 and Δ+0.54 mm^2; 2-mm pss, Δ+0.65 and Δ+0.58 mm^2; vessel area change and plaque area change respectively) without affecting the lumen size (1-mm pss, Δ-0.02 mm^2; 2-mm pss, Δ+0.07 mm^2 in lumen area change), while in the following 3 subsegments overcompensation was observed, that is the vessel wall grew more than the plaque (3-mm pss, Δ+1.98 and Δ+1.18 mm^2; 4-mm pss, Δ+1.32 and Δ+0.12 mm^2; 5-mm pss, Δ+0.54 and Δ+0.14 in vessel area change and plaque area change respectively), resulting in an increase in lumen size (3-mm pss, Δ+0.81 mm^2; 4-mm pss, Δ+1.21 mm^2; and 5-mm pss, Δ+0.69 mm^2). At the distal edge, overcompensation was observed in all 5 subsegments, resulting in an increase in lumen size (1-mm dss, Δ+0.88; Δ+0.23 and Δ+1.35 mm^2; 2-mm dss, Δ+0.67; Δ+0.04 and Δ+1.24 mm^2; 3-mm dss, Δ+0.17; Δ-0.63 and Δ+1.72 mm^2; 4-mm dss, Δ+0.51; Δ-0.36 and Δ+1.42 mm^2; 5-mm dss, Δ+0.63; Δ-0.10 and Δ+1.61mm^2 in vessel, plaque and lumen area change respectively).

At 6-month follow-up, the percentage of fibrofatty tissue increased in all subsegments, while fibrous tissue showed a more heterogeneous behavior, with calcified tissue and necrotic core being decreased throughout the ten subsegments analyzed. (Figure).

DISCUSSION

The main findings of this study were the following: *a)* at the proximal and distal edge, a serial expansive vascular remodeling was observed, with an increase in mean vessel area and mean lumen area of the entire edge from baseline to follow-up; *b)* in the first 3 subsegments adjacent to the proximal part of the stent the most prominent increase in mean plaque area was observed. This is in line with the results of the Taxus II and IV studies[11,15]; and *c)* overall, in the proximal and distal segment a significant increase of fibrofatty tissue was observed, while a decrease of calcified tissue and necrotic core over time was present.

The serial changes in tissue composition at the edges of the stent could vary depending on the location (proximal vs distal edge), shear stress conditions,[16] morphological baseline characteristics (degree of obstruction) of the segment as well as baseline tissue composition. Last but not least, the degree of vessel wall injury after dilatation plays a role.[17] In animal and human pathological studies the response-to-injury process after stenting has been extensively described.[10] Restenosis occurs secondary to accumulation of smooth muscle cells and extracellular matrix, which consists of proteoglycans, hyaluronan and collagen (Type I and III). This extracellular matrix modulates neointimal growth and remodeling.[10] The IVUS-RFD tissue type that correlates with extracellular matrix is the fibro-fatty tissue, which happened to be the one that mostly increased in this study and, positive remodeling was also observed at both stent edges at 6 months. Serial remodeling has been proposed as the best approach to evaluate the geometrical vessel wall changes[18]. In this regard other previous Taxus® stent studies have described this phenomenon at the edges. In particular, in TAXUS II[11] a positive remodeling was only observed at the distal edge in both slow and moderate release Taxus group due to an increase in plaque size and hardly not change in lumen size; while in TAXUS IV[15] almost no change was observed in vessel size at the proximal edge and a trend towards negative remodeling was observed at the distal edge. It is difficult to put into perspective these three studies, since they all have different sample size, in TAXUS IV authors acknowledged potential selection bias. So, although this study has a small sample size; a more complete characterization of the serial changes has been achieved.

In the present study, necrotic core rich areas were left unstented (proximal edge 17% [13.5%] and distal

edge 18.5% [16.5%]), however no stent thrombosis has been observed in this small cohort of patients. Proposed pathological mechanisms of stent thrombosis are stenting of necrotic core-rich plaques with extensive tissue prolapse and plaque disruption in the proximity of the stented arterial segment.[19,20] IVUS-RFD is not only able to characterize necrotic core with high sensitivity and specificity,[14] it also provides geometrical analysis of each frame, allowing us to have the combined assessment of necrotic core and plaque size. Thus, pre-stenting imaging using IVUS-RFD can give us an insight into the extent of plaque and necrotic core within and beyond the intended stenting segment. This latter assessment is important since stenting has been lately performed from "normal to normal" arterial segments in angiography; however, disruption of adjacent necrotic core-rich areas that are angiographically disease-free should be avoided. Indeed, it has been reported that incomplete coverage of coronary atherosclerotic plaques with drug-eluting stents may impact on long-term clinical events, especially in necrotic-core rich plaques.[19] Nevertheless, in this study, a decrease in necrotic core was showed at both edges at follow-up. Whether this is related to the presence of a stent or even more to the drug type eluted on the stent remains to be elucidated.

The limitations of this study are various. Firstly, only a small cohort of patients has been included, since the study was considered mainly exploratory and without formal statistical hypothesis. Secondly, it would have been ideal to study completely the stent segment plus the edge effects, however as mentioned earlier, there is no validation of the tissue characterization behind the stent struts which may themselves interfere with the process of ultrasound backscattering of the tissue located behind the struts. Six-month follow-up may be a relatively short period of time to fully evaluate the tissue changes at the edges of the stent considering the fact that longer angiographic follow-up has been suggested to better evaluate the vascular responses at these locations.

CONCLUSIONS

Serial expansive vascular remodeling was observed at the proximal and distal stent edges, to accommodate a tissue growth mainly due to an increase in fibrofatty tissue.

REFERENCES

1. Serruys PW, Kutryk MJ, Ong AT. Coronary-artery stents. N Engl J Med. 2006;354:483-95.
2. McFadden EP, Stabile E, Regar E, Cheneau E, Ong AT, Kinnaird T, et al. Late thrombosis in drug-eluting coronary stents after discontinuation of antiplatelet therapy. Lancet. 2004;364: 1519-21.
3. Spaulding C, Daemen J, Boersma E, Cutlip DE, Serruys PW. A pooled analysis of data comparing sirolimus-eluting stents with bare-metal stents. N Engl J Med. 2007;356:989-97.
4. Stone GW, Moses JW, Ellis SG, Schofer J, Dawkins KD, Morice MC, et al. Safety and efficacy of sirolimus- and paclitaxel-eluting coronary stents. N Engl J Med. 2007;356:998-1008.
5. Kastrati A, Mehilli J, Pache J, Kaiser C, Valgimigli M, Kelbaek H, et al. Analysis of 14 trials comparing sirolimus-eluting stents with bare-metal stents. N Engl J Med. 2007;356:1030-9.
6. Lagerqvist B, James SK, Stenestrand U, Lindback J, Nilsson T, Wallentin L. Long-term outcomes with drug-eluting stents versus bare-metal stents in Sweden. N Engl J Med. 2007;356:1009-19.
7. Mauri L, Hsieh WH, Massaro JM, Ho KK, D'Agostino R, Cutlip DE. Stent thrombosis in randomized clinical trials of drug-eluting stents. N Engl J Med. 2007;356:1020-9.
8. Dibra A, Kastrati A, Mehilli J, Pache J, Schuhlen H, von Beckerath N, et al. Paclitaxel-eluting or sirolimus-eluting stents to prevent restenosis in diabetic patients. N Engl J Med. 2005;353:663-70.
9. Windecker S, Remondino A, Eberli FR, Juni P, Raber L, Wenaweser P, et al. Sirolimus-eluting and paclitaxel-eluting stents for coronary revascularization. N Engl J Med. 2005; 353:653-62.
10. Farb A, Kolodgie FD, Hwang JY, Burke AP, Tefera K, Weber DK, et al. Extracellular matrix changes in stented human coronary arteries. Circulation. 2004;110:940-7.
11. Serruys PW, Degertekin M, Tanabe K, Russell ME, Guagliumi G, Webb J, et al. Vascular responses at proximal and distal edges of paclitaxel-eluting stents: serial intravascular ultrasound analysis from the TAXUS II trial. Circulation. 2004;109:627-33.
12. Nair A, Kuban BD, Tuzcu EM, Schoenhagen P, Nissen SE, Vince DG. Coronary plaque classification with intravascular ultrasound radiofrequency data analysis. Circulation. 2002; 106:2200-6.
13. Nasu K, Tsuchikane E, Katoh O, Vince DG, Virmani R, Surmely JF, et al. Accuracy of in vivo coronary plaque morphology assessment: a validation study of in vivo virtual histology compared with in vitro histopathology. J Am Coll Cardiol. 2006;47:2405-12.
14. Nair A MP, Kuban BD, Vince DG. Automated coronary plaque characterization with intravascular ultrasound backscatter: ex vivo validation. Eurointervention. 2007;3:113-30.
15. Weissman NJ, Koglin J, Cox DA, Hermiller J, O'Shaughnessy C, Mann JT, et al. Polymer-based paclitaxel-eluting stents reduce in-stent neointimal tissue proliferation: a serial volumetric intravascular ultrasound analysis from the TAXUS-IV trial. J Am Coll Cardiol. 2005;45:1201-5.
16. Wentzel JJ, Gijsen FJ, Stergiopulos N, Serruys PW, Slager CJ, Krams R. Shear stress, vascular remodeling and neointimal formation. J Biomech. 2003;36:681-8.
17. Wilcox JN, Okamoto EI, Nakahara KI, Vinten-Johansen J. Perivascular responses after angioplasty which may contribute to postangioplasty restenosis: a role for circulating myofibroblast precursors? Ann N Y Acad Sci. 2001;947:68-90.
18. Mintz GS, Nissen SE, Anderson WD, Bailey SR, Erbel R, Fitzgerald PJ, et al. American College of Cardiology Clinical Expert Consensus Document on Standards for Acquisition, Measurement and Reporting of Intravascular Ultrasound Studies (IVUS). A report of the American College of Cardiology Task Force on Clinical Expert Consensus Documents. J Am Coll Cardiol. 2001;37:1478-92.

19. Farb A, Burke AP, Kolodgie FD, Virmani R. Pathological mechanisms of fatal late coronary stent thrombosis in humans. Circulation. 2003;108:1701-6.

20. Finn AV, Nakazawa G, Joner M, Kolodgie FD, Mont EK, Gold HK, et al. Vascular responses to drug eluting stents: importance of delayed healing. Arterioscler Thromb Vasc Biol. 2007;27:1500-10.